The EMBO Journal vol.7 no.5 pp.1549 - 1554, 1988

Three-dimensional structure of the regular surface glycoprotein layer of *Halobacterium volcanii* from the Dead Sea

Martin Kessel, Ivo Wildhaber[1], Simone Cohen and Wolfgang Baumeister[1]

Department of Membrane and Ultrastructure Research, Hadassah Medical School, The Hebrew University, PO Box 1172, Jerusalem 91-010, Israel, and [1]Max-Planck Institut für Biochemie, D-8033 Martinsried, FRG

Communicated by D.Oesterhelt

A three-dimensional reconstruction from electron micrographs of negatively stained cell envelopes of *Halobacterium volcanii* has revealed the structure of the surface glycoprotein to a resolution of 2 nm. The glycoprotein is arranged on a p6 lattice with a lattice constant of 16.8 nm. It forms 4.5 nm high, dome-shaped, morphological complexes with a narrow pore at the apex opening into a 'funnel' towards the cell membrane. The polarity of the structure was derived from freeze-etching experiments and 'edge' views. Six radial protrusions emanate from each morphological complex and join around the 3-fold axis to provide lateral connectivity. Using the primary structure of the surface glycoprotein of the closely related species *Halobacterium halobium* (Lechner and Sumper, 1987) and the cell envelope profile from a previous X-ray analysis of the same species (Blaurock *et al.*, 1976) we have integrated our reconstruction into a model of halobacterial cell envelope.

Key words: electron microscopy/halobacterial cell wall/glycoprotein/three-dimensional reconstruction

Introduction

Extreme or moderate halophiles of the Halobacteria family with a characteristic lack of a peptidoglycan in their cell wall are grouped among the Archaebacteria (Woese and Fox, 1977). An early electron microscopy study of a shadow cast preparation of *Halobacterium halobium* by Houwink (1956), showed the outer surface of the wall to be composed of an hexagonal array of morphological units with a spacing of ~16.8 nm. Thin sectioning studies of a number of Halobacteria have shown an ~17 nm thick wall layer external to the cell membrane (Kirk and Ginzburg, 1972; Robertson *et al.*, 1982; Steensland and Larsen, 1969; Stoeckenius and Rowen, 1967; Usukura *et al.*, 1980). Depending upon fixation procedures the wall shows a scalloped periodicity similar to that seen in shadow cast preparations. Examination of isolated cell envelope preparations by negative staining showed a honeycomb appearance of an hexagonal arrangement of stain accumulations at an equivalent spacing to that seen in shadow casting (D'Aoust and Kushner, 1972). A brief description of the negative stain appearance of envelopes of *Halobacterium volcanii* (Kessel *et al.*, 1987) has shown the morphological units to comprise six subunits in a hexagonal arrangement.

Mescher and Strominger (1976) were the first to show that the surface glycoprotein of Halobacteria is essential for maintaining the rod shape of the cell. Moreover, the exposed location of the wall at the cell–environment interface suggests a vital role for this structure in the survival of these organisms at extreme salt concentrations. In spite of the obvious importance of the surface glycoprotein array our knowledge of the molecular organization of halobacterial surface layers is still rather meagre, which is in contrast to another characteristic cell envelope component of Halobacteria, the bacteriorhodopsin containing purple membrane, where in a relatively short period of time a plethora of biochemical and biophysical data has been accumulated (Stoeckenius and Bogomolni, 1982). Recently, however, after elucidating the nature and pathway of the glycosylation and the demonstration that the glycoprotein contains two different types of sulfated saccharides linked to the protein via two unique types of *N*-glycosidic linkages and an *O*-linked disaccharide (Paul and Wieland, 1987; Wieland *et al.*, 1980), the primary structure of the surface glycoprotein in *H.halobium* has been established by cloning and sequencing its gene (Lechner and Sumper, 1987).

Electron microscopy of halobacteria has always been hampered by the high salt concentration required to maintain the integrity of the regular surface arrays. We have recently found that cell envelopes of a moderate halophile from the Dead Sea, *H.volcanii* (Mullakhanbai and Larsen, 1975), which requires a growth medium containing 2.14 M NaCl and 0.25 M $MgCl_2$, can be maintained intact in concentrations of divalent cations as low as 10 mM $CaCl_2$ alone (Cohen, 1987; Kessel *et al.*, 1986). The surface details of cell envelopes maintained under these conditions appear after examination by air- or freeze-drying followed by heavy metal shadowing or by negative staining to be identical to the surface of freeze fractured whole cells. We are therefore confident that the envelope structure has remained intact at least to the level of resolution determined in our reconstruction. These preparations have provided us with areas of images of sufficiently high quality to present the first three-dimensional reconstruction of the surface glycoprotein of a *Halobacterium*. The reconstruction at a resolution of 2 nm shows a distinct funnel shaped pore spanning the 4.5 nm width of the layer. The pore is dome shaped and almost occluded at one end and has a wide opening at the other. Considerations are presented in support of the dome end facing outward towards the medium and the wide opening directed towards the cell membrane. The information combined from the three-dimensional reconstruction presented here and sequence data from the closely related species, *H.halobium*, is integrated into a model of the cell envelope.

Results

Figure 1a is an electron micrograph of a negatively stained (nominally untilted) *H.volcanii* envelope suspended in

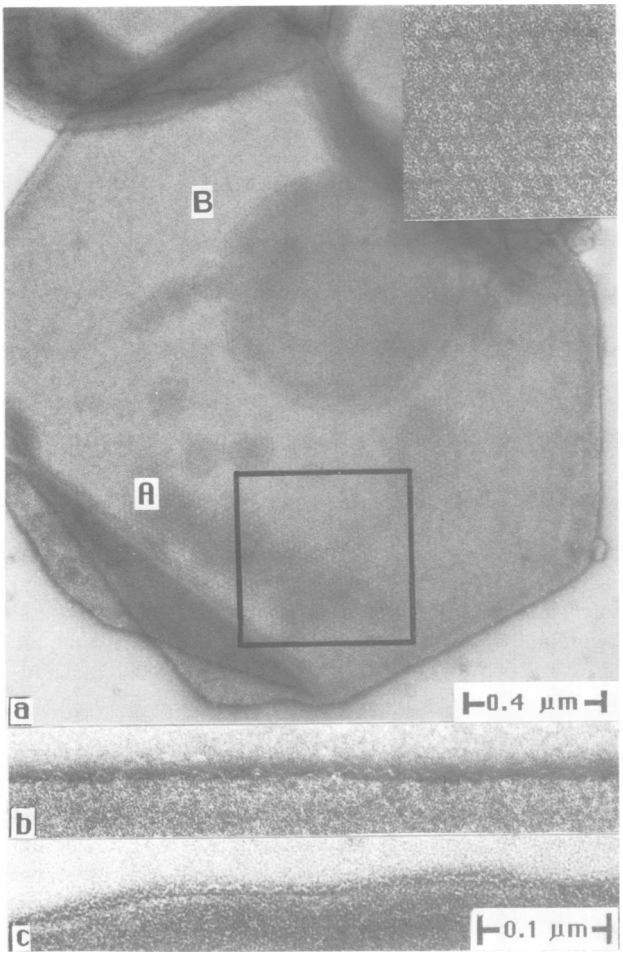

Fig. 1. (**a**) Cell envelope of *H.volcanii*, negatively stained with 0.75% uranyl formate. The boxed area (shown in part at higher magnification in the inset) was that used for the three-dimensional reconstruction. Different areas in the micrograph (A and B) show different staining patterns: A is an area with morphological units well embedded in stain and B is an area with stain accumulating only at the centre of the morphological unit. (**b**) and (**c**) comparative edge views of negatively stained cell envelopes of *H.volcanii* (b) and *H.halobium* (c) showing similar rows of adjacent parabolas 4.5 nm in height.

10 mM $CaCl_2$. We see the typical angular shape of the envelope and the variability in the level of stain embedding demonstrating regions which clearly show the hexagonal arrangement of morphological units, regions which appear almost featureless and regions with the honeycomb pattern, described earlier. These different regions appear to merge one into another. Optical diffraction however, reveals that the envelope comprises a coherent lattice covering the entire surface (with a centre to centre spacing between morphological units of 16.8 nm), instead of being composed of a patchy, 'polycrystalline' surface layer as the micrographs might suggest at a first glance. Moreover, averages from the different regions show basically the same features at slightly differing degrees of resolution.

Despite the fact that we are dealing with collapsed envelopes, almost exclusively only one of the two layers (top or bottom) appears to have been sufficiently embedded in negative stain to show up clearly. The correlation averages of untilted projections, typically including 200 motifs, show a ring structure with a 5 nm wide, stain accumulating centre and a 5 nm wide, stain-excluding, ring resolved into six distinct globular domains each ~ 3 nm in diameter (Figure 2a). The structure has a clear p6 symmetry. A radial arm extends from each of the ring domains in a pin wheel orientation when viewed in projection, and the arms from adjacent rings seem to join near the 3-fold crystallographic axis. Hence the structure can be classified as M_6C_3 according to the notation proposed by Saxton and Baumeister (1986). A second but smaller protrusion directed towards the 2-fold axis appears to end blindly. At a lower resolution this 'arm' coalesces with the radial arm.

Figure 2b shows three vertical sections through the three-dimensional structure (directions t, m and b in Figure 2a). The vertical sections reveal the distribution of mass (stain exclusion) within the height of the 4.5 nm included in the reconstruction. A thickness of 4.5 nm for the glycoprotein surface layer is in agreement with X-ray diffraction data obtained with *H.halobium* cell envelopes (Blaurock *et al.*, 1976). In a note added in proof these authors used their data to calculate the molecular volume of the unit cell concluding that the 780 nm^3 unit cell can accomodate 'just over three

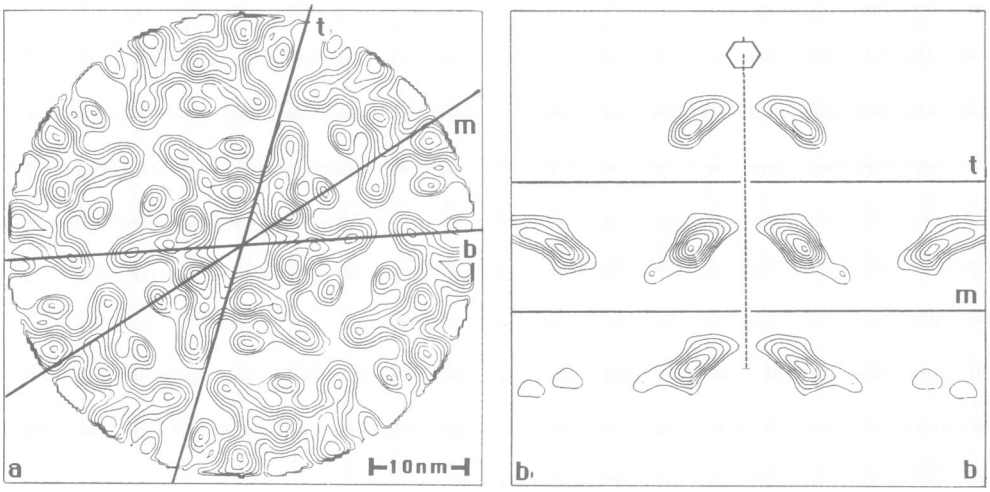

Fig. 2. Contour plot from a correlation average of an untilted specimen (**a**) and from vertical sections through the three-dimensional structure (**b**). The vertical sections (from top to bottom) correspond to the lines indicated with t, m and b in (a). The 6-fold axis is indicated.

molecules' which is not commensurate with the p6 symmetry we find requiring (at least) six monomers per unit cell. Their calculation was however based on an apparent mol. wt for the glycoprotein monomer of 200 kd, which grossly deviates from the actual mol. wt recently derived from the sequence data [86 kd (Lechner and Sumper, 1987)]. The revised mol.

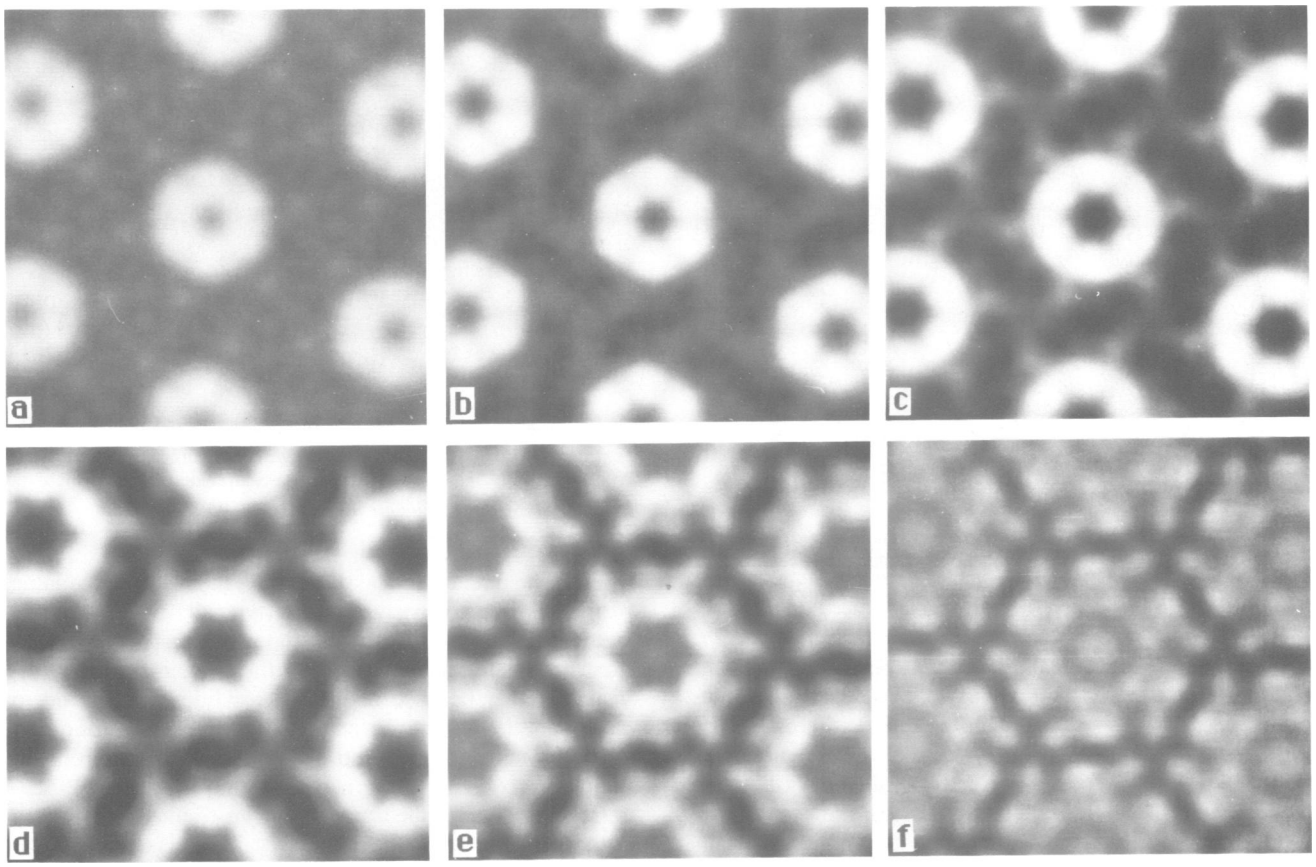

Fig. 3. Horizontal sections through the three-dimensional structure with 0.6 nm increments. The sections (**a**–**f**) begin 1.6 nm above (a) and extend to 1.6 nm below the centre of the layer (f).

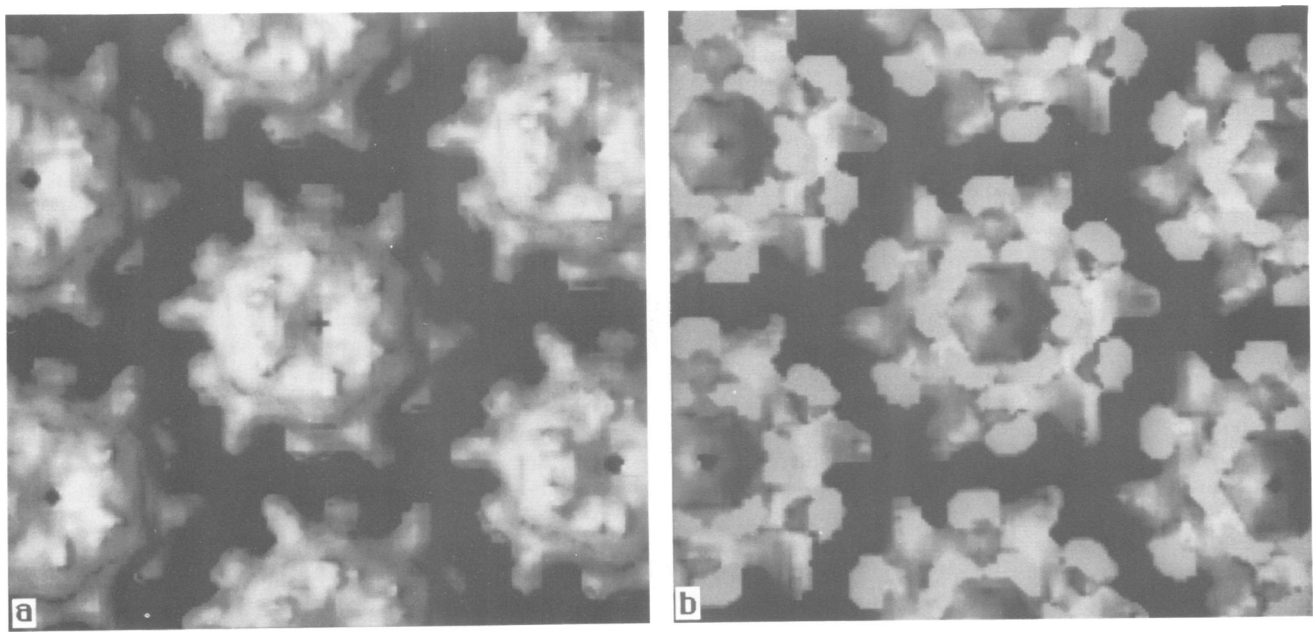

Fig. 4. Computer generated shaded view of the three-dimensional reconstruction of the morphological unit viewed (**a**) from the outer surface and (**b**) from the inner surface.

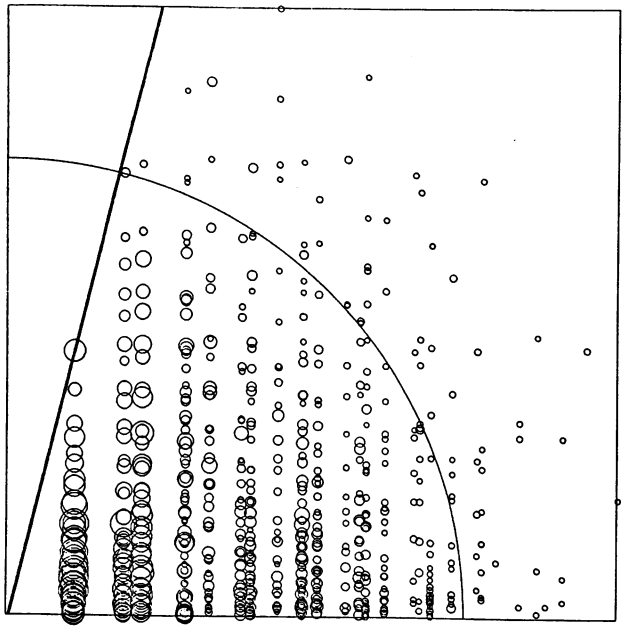

Fig. 5. Spatial distribution of data in Fourier space. The area enclosed by each circle is proportional to the modulus of the corresponding Fourier coefficient. The curve respresents a 2 nm resolution level and the tilt angle of 76° defines the data included in the reconstruction.

wt allows us to reconcile all pertinent experimental data. In Figure 2b the top section does not pass through either the radial arms or the mass between the arms, whereas in the middle and at the bottom section both of these regions are sectioned, thereby accentuating the lateral extension of the stain excluding region in the lower part of the reconstruction. The pore is seen as a funnel shaped region of stain accumulation extending downwards from a narrow opening just below the rim of the pore almost at the apex of a dome.

Figure 3 shows a composite of z-sections through the three-dimensional volume of 0.6 nm increments. A simple 6-fold arrangement of globular domains appears in the first sections. At a z-distance of 2.7 nm from the first section there is evidence for the radial arms which determine the handedness. The ring structure becomes wider towards the bottom such that neighbouring morphological complexes come into closer proximity and the mass disposition within the unit cell shows an increasing complexity. The most prominent feature in the last slices containing significant density are the protrusions pointing towards the 2-fold axes.

Figure 4 shows views of the two surfaces of the layer obtained by 'surface shading'. In Figure 4a we see a distinct dome shape with six protrusions and a small opening in a depression just below the apex. The radial arms are seen at the base of the dome, each directed towards the 3-fold axis and adjacent to the interstitial domains which appear to end blindly near the 2-fold axis. In Figure 4b we see the wide opening of the pore with the ring comprising six domains from which the radial arms appear to emanate. The interstitial domains located midway between the radial arms project downwards. The molecular volume displayed in the surface shading model represents only 45% of the volume expected for a mol. wt of 86 kd per monomer (Lechner and Sumper, 1987) and a protein density of 1.33 g/cm^3. Even when taking into account that, as a consequence of restrictive thresholding for the sake of clarity, the molecular volume of models is notoriously too low (typically 50−80%) this figure is somewhat surprising. It may be taken as an indication that a substantial portion of the protein remained invisible, either because of local flexibilities which tend to cancel out the respective features upon averaging, or a part of the protein is buried in the membrane and therefore remains inaccessible to the negative stain (see below).

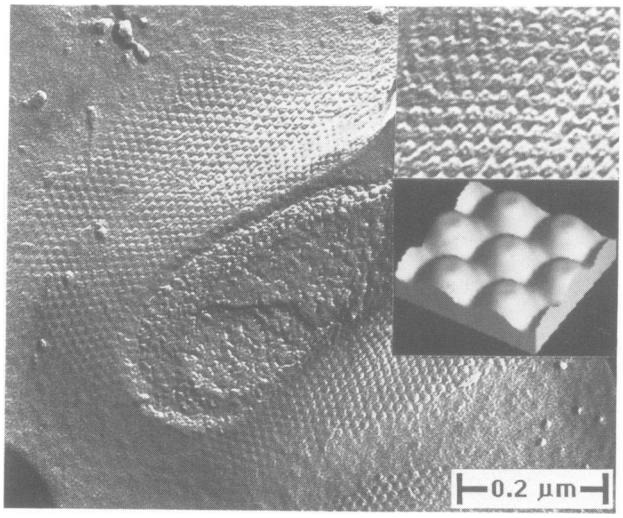

Fig. 6. Deep-etched specimen of a *H.volcanii* cell showing the hexagonally ordered cell surface layer. Inset: magnified area and relief reconstruction of the outer surface of the S-layer derived from the freeze-etched preparation.

Determination of the actual tilt angles resulted in a tilt correction of 2° from the nominal values. The highest tilt achieved was therefore 76°. The specimen inclination to the direction of the tilt axis was 1.5°. Figure 5 shows the distribution of the data in Fourier space where each area enclosed by each circle is proportional to the modulus of the corresponding Fourier coefficient. The data clearly show the information contributing to the structure at the highest tilt angle thus reducing the problem of the missing cone.

Discussion

There are two lines of evidence which make it clear that the narrow end of the funnel, i.e. the dome, points to the outside of the cell and, consequently, the wide opening of the funnel is directed towards the cell membrane.

(i) A surface reconstruction from an area of the cell surface revealed by freeze etching (Figure 6) confirms the overall dome shape of the morphological units of the surface glycoprotein; resolution is not sufficient, however, to reveal any clear depression on the 6-fold axis, i.e. the narrow opening of the funnel.

(ii) Close examination of the folded-over edges of the wall in Figure 1b reveals side views appearing as a string of parabolas which are consistent with the dome end facing the exterior. The overall design of the *Halobacterium* surface glycoprotein and its orientation in the cell envelope are not unusual amongst archaebacteria. *Sulfolobus solfataricus* which is found in extreme habitats of high temperature and low pH also has a dome-shaped surface glycoprotein, similar in its proportions and with a narrow outlet on the outer

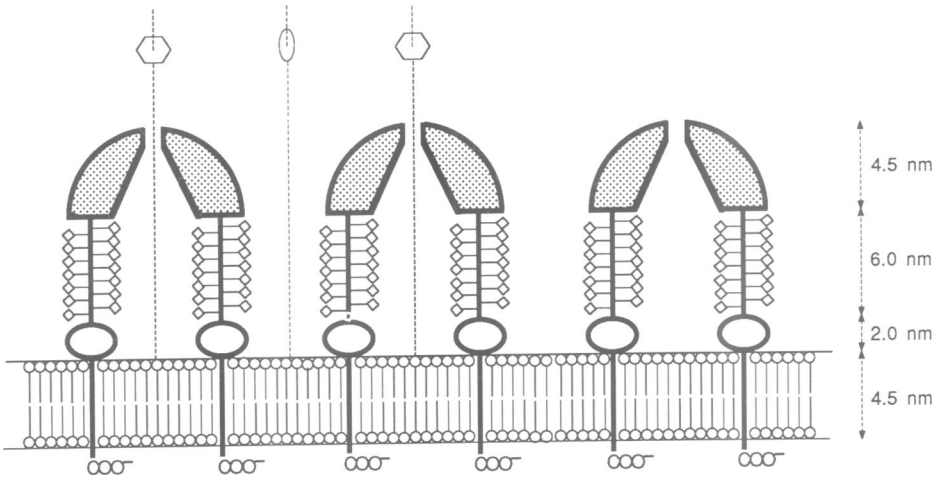

Fig. 7. Schematic diagram summarizing the available structural information on the *Halobacterium* cell envelope from: (i) X-ray studies of the envelopes (Blaurock *et al.*, 1976), (ii) the primary structure of the surface glycoprotein (Lechner and Sumper, 1987), and (iii) the three-dimensional structure described in this communication. The three-dimensional structure determined by electron microscopy depicts only the upper dome-shaped region of the structure which is separated from the cell membrane by the 'spacer elements'. As indicated by the crystallographic symbols the section runs from 6-fold to 6-fold axis via the 2-fold axis.

surface; the wide side of the funnel is directed towards the cell membrane (Prüschenk and Baumeister, 1988).

To understand the functional implications of such a configuration it is important to examine the surface glycoprotein layer in relation to other components of the cell envelope. In order to be able to combine in a general model the structural results obtained in this study for *H.volcanii*, with the published X-ray (Blaurock *et al.*, 1976), chemical and sequence data for *H.halobium* (Lechner and Sumper, 1987), we have compared the main features of the cell surfaces of the two species and the results may be summarized as follows.

(i) The periodic surface arrays of *H.halobium* R_1M_1 and *H.volcanii* have identical lattice constants of 16.8 nm.

(ii) Examination of the cell surface of *H.halobium* by heavy metal shadowing and surface relief reconstruction has revealed an outward-facing dome shape of the morphological unit with a small central depression very similar to that observed in *H.volcanii*.

(iii) Despite the greater difficulty in obtaining good negatively stained envelopes of *H.halobium* due to the high concentration of NaCl necessary to maintain the integrity of the lattice, we were able to obtain preparations showing in projection the same disposition of mass centres in the core as found in *H.volcanii*. At the resolution attained so far with *H.halobium* it is not clear whether this similarity also pertains to the connecting domains between morphological units. Edge views of negatively stained preparations of envelopes of *H.halobium* appear virtually identical to those observed with *H.volcanii* (Figures 1b and c).

Therefore, despite the fact that *H.halobium* and *H.volcanii* are found in nature under different salt conditions (4.0 M NaCl and 2.14 M NaCl + 0.25 M $MgCl_2$, respectively) and have a different overall shape (a rod versus a pleomorphic shape), the basic structural features of their cell surfaces seem to be identical, at least to the 2.5 nm resolution level so far attained.

These findings justify combining the chemical data available for *H.halobium* and the structural information obtained in the course of this electron microscope study with *H.volcanii*, into a model of the spatial organization of the halobacterial cell surface.

Blaurock *et al.* (1976) describe a cell envelope profile where the surface protein layer (approximated with an 'inverted-parabola shape') is separated from a second, 2 nm thick (inner) protein layer which is directly apposed to the cell membrane, by a 6.5 nm wide space with an electron density close to that of the suspending medium. Again, such an interspace which may be regarded as analogous to the periplasmic space of the gram-negative eubacteria, is not unusual amongst archaebacteria. In *Thermoproteus tenax* the surface layer is ~25 nm away from the cell membrane (Wildhaber and Baumeister, 1987), like a roof resting on pillars. Also in *Sulfolobus* there is evidence from electron micrographs of thin sections (Wildhaber *et al.*, in preparation) of a cell envelope profile closely resembling that of the *Halobacterium* cell wall. A fairly constant distance separating the surface layer from the cell membrane requires the presence of some kind of spacer element. Such a spacer can either be an integral element of the surface glycoprotein, as in *T.tenax*, or it may be provided by an accessory molecular species. The spacer should, with its distal end also serve as a membrane anchor. In the case of *H.halobium* the amino acids sequence suggests that a hydrophobic stretch of 21 amino acids near the C-terminus (positions 795–815) serves as a membrane anchor (Lechner and Sumper, 1987), which would imply that the spacer element is also an integral part of the surface glycoprotein. Amino acids 755–774 with their unusual clustering of glycosylated threonine residues could provide the spacer element, thus leaving amino acids 775–794 to create a small globular domain (the 'inner' protein layer) next to the outer surface of the cell membrane. The spacer domain, which is presumed to emanate from the blindly ending domain protruding towards the 2-fold axis, is too small to be resolved in our reconstruction. It is also clear that the membrane anchor remains invisible. This accounts at least partly for the deficit in the reconstructed molecular volume mentioned above.

In a discussion on the cellular location of halobacterial glycoprotein synthesis Sumper (1987) presents evidence that

the glycosylation reaction takes place at the extracellular surface of the cell membrane. The model presented in Figure 7 provides a plausible structural basis for the existence of a compartment which could accommodate the enzymes involved.

The results presented here give us for the first time an insight into the spatial organization of the glycoprotein surface layer of a representative species of the Halobacteria. Figure 7 summarizes the information from our three-dimensional reconstruction, the X-ray studies and the primary structure and incorporates them into a model for the organization of the *Halobacterium* cell envelope.

Materials and methods

Envelope preparation

Cells of *H.volcanii* were grown to late logarithmic phase and washed twice in a solution of 2.14 M NaCl and 0.25 M $McCl_2$ by centrifugation for 20 s in an Eppendorf centrifuge. The cells were suspended in the above solution and frozen by plunging the Eppendorf tube containing the cell suspension into liquid nitrogen until bubbling ceased. The frozen cells were allowed to thaw at room temperature. The broken cell suspension was incubated with 10 μg/ml of DNase for 1 h at 37°C, and then centrifuged for 15 s to remove unbroken cells and other debris. The resulting cell envelope suspension was washed twice in 2.14 M NaCl and 0.25 M $MgCl_2$ by centrifugation for 7 min and the pellet resuspended in 10 mM $CaCl_2$ only after all the supernatant had been thoroughly removed.

For comparative purposes we examined cell envelopes of *H.halobium* strain R_1M_1. This strain was made available to us by D.Oesterhelt.

Electron Microscopy

A 5 ml drop of the envelope preparation was placed on a freshly glow-discharged, carbon coated copper grid for 30 s and removed by touching with filter paper. The grid was then inverted on two successive drops of water for 25 s and touched to a drop of freshly prepared 0.75% uranyl formate for 30 s. Excess stain was removed from the grid by touching with filter paper followed by gentle suction with a finely drawn Pasteur pipette.

Specimens were examined in a Philips EM420 electron microscope operating at 100 kV using the unlimited tilt specimen holder of Chalcroft and Davey (1984). A tilt series of nominal tilt angles from 0 to 78.6° was recorded with tilt increments decreasing in proportion to cos ψ (Saxton *et al.*, 1984). The tilt series was recorded from the same area of the envelope and the cumulative electron dose was 60 000 e/nm^2. Possible radiation damage was monitored by comparing micrographs at zero tilt taken at the beginning and end of the series. Micrographs were recorded at a magnification of ×35 000 on Kodak film SO-163 at a defocus of ~400 nm.

Images were examined in an optical diffractometer to select the areas with an optimal preservation of crystalline order, and in order to monitor defocus and astigmatism. Selected areas corresponding to a 512 × 512 pixel array were densitometered at a step size of 20 μm equivalent to a sampling of 0.57 nm per pixel.

Image processing

Reconstructions were carried out using the SEMPER system (Saxton *et al.*, 1979), and the EM system (Hegerl and Altbauer, 1982). All projections were subjected to correlation averaging using the method of Saxton and Baumeister (1982). Three-dimensional reconstruction was performed (after correction of the tilt angles) using the hybrid real space/Fourier space approach (Saxton *et al.*, 1984). For determining the sidedness of the layer, surface relief reconstructions were performed applying the method described by Guckenberger (1985) to micrographs of replicas from freeze-etching experiments. Surface shading of the three-dimensional model was performed using the method of Saxton (1985).

Acknowledgements

M.K. wishes to acknowledge the receipt of a short-term Fellowship from EMBO. The original negative staining experiments were carried out with Drs U.Aebi and E.L.Buhle,Jr at the Johns Hopkins University School of Medicine, Baltimore, MD, and freeze etching was performed by Dr C.Franzini-Armstrong, Department of Biology, University of Pennsylvania, Philadelphia, PA. We wish to thank Drs D.Oesterhelt and M.Sumper for critical reading of the manuscript.

References

Blaurock,A., Stoeckenius,W., Oesterhelt,D. and Scherphof,G. (1976) *J. Cell Biol.*, **71**, 1–22.
D'Aoust,J.-Y. and Kushner,D.J. (1972) *Can. J. Microbiol.*, **18**, 1767–1768.
Chalcroft,J. and Davey,C.L. (1984) *J. Microsc. (Oxford)*, **134**, 41–48.
Cohen,S. (1987) Ph.D. Thesis, Hebrew University, Jerusalem.
Guckenberger,R. (1985) *Ultramicroscopy*, **16**, 357–370.
Hegerl,R. and Altbauer,A. (1982) *Ultramicroscopy*, **9**, 109–116.
Houwink,A.L. (1956) *J. Gen. Microbiol.*, **15**, 146–150.
Kessel,M., Buhle,E.L., Jr., Cohen,S. and Aebi,U. (1986) Proc. XIth Int. Cong. on Electron Microscopy, Kyoto, *J. Microsc.*, **35**, (supplement) 2471–2472.
Kirk,G. and Ginzburg,M. (1972) *J. Ultrastruc. Res.*, **41**, 80–94.
Lechner,J. and Sumper,M. (1987) *J. Biol. Chem.*, **262**, 9724–9729.
Mescher,M.F. and Strominger,J.L. (1976) *J. Biol. Chem.*, **251**, 2005–2014.
Mullakhanbai,M.F. and Larsen,H. (1975) *Arch. Microbiol.*, **104**, 207–214.
Paul,G. and Wieland,F. (1987) *J. Biol. Chem.*, **262**, 9587–9593.
Prüschenk,R. and Baumeister,W. (1988) *Eur. J. Cell Biol.* **45**, 185–191.
Robertson,J.D., Schreil,W. and Reedy,M. (1982) *J. Ultrastruc. Res.*, **80**, 148–162.
Saxton,W.O. (1985) *Ultramicroscopy*, **16**, 387–394.
Saxton,W.O., Pitt,T.J. and Horner,M. (1979) *Ultramicrosc.*, **4**, 343–354.
Saxton,W.O. and Baumeister,W. (1982) *J. Microsc. (Oxford)*, **127**, 127–128.
Saxton,W.O., Baumeister,W. and Hahn,M. (1984) *Ultramicroscopy*, **13**, 57–70.
Saxton,W.O. and Baumeister,W. (1986) *J. Mol. Biol.*, **187**, 251–253.
Steensland,H. and Larsen,H. (1969) *J. Gen. Microbiol.*, **55**, 325–336.
Stoeckenius,W. and Rowen,R. (1967) *J. Cell Biol.*, **34**, 365–393.
Stoeckenius,W. and Bogomolni,R.A. (1982) *Annu. Rev. Biochem.*, **52**, 587–615.
Sumper,M. (1987) *Biochem. Biophys. Acta*, **906**, 69–79.
Usukura,J., Yamada,E., Tokunaga,F. and Yoshizawa,T. (1980) *J. Ultrastruc. Res.*, **70**, 204–219.
Wieland,F., Dompert,W., Bernhardt,G. and Sumper,M. (1980) *FEBS Lett.*, **120**, 110–114.
Wildhaber,I. and Baumeister,W. (1987) *EMBO J.*, **6**, 1475–1480.
Woese,C. and Fox,G.E. (1977) *Proc. Natl. Acad. Sci. USA*, **74**, 5088–5090.

Received on January 27, 1988; revised on February 15, 1988